scientific reports

Check for updates

OPEN

Polydatin exerts therapeutic effects on myelodysplastic syndrome by inhibiting the protein expression of oncogenes via hypermethylation in vitro

Qingbing Zhou[1,4], Yuanbin Liang[1,4], Ruofan Chen[1,4], Hongzhi Wang[2], Qiuyue Guo[2], Li Liu[2], Xiaobo Zhu[3✉] & Fengqin Xu[1✉]

DNA methylation plays a critical role in myelodysplastic syndrome (MDS). Here, we aimed to observe the effects of polydatin (PD) on DNA methylation in MDS cells on a genome-wide scale and explore the underlying mechanisms, providing new evidence for PD as a novel hypermethylation agent. We used the Gene Expression Omnibus (GEO) online database to evaluate the DNA methylation characteristics of MDS patients. A Human Methylation 850 K BeadChip was used to evaluate the effects of PD on DNA methylation in SKM-1 cells. Western blotting (WB) was used to observe changes in the expression of related proteins. Cytoscape was used to determine the key genes that were hypermethylated by PD. The therapeutic effects were evaluated using flow cytometry experiment and a cell counting kit-8 (CCK-8) assay in vitro. Data from the GEO online database revealed that aberrant gene hypomethylation plays an important role in MDS. In MDS cells, 448 genes (71.91%) were hypermethylated following PD treatment. These hypermethylated genes are related to cancer-related signaling pathways. Moreover, key hypermethylated genes, including PIK3CA, ITPR3 and SPOPL, were identified, and these three genes are all oncogenes. Most importantly, PD decreased the protein expression of the above three oncogenes. Finally, we found that PD could inhibit the proliferation of MDS cells, arrest them in the S phase and induce their apoptosis. Our findings demonstrated that PD has therapeutic effects on MDS by inhibiting the protein expression of oncogenes via hypermethylation in vitro, indicating that PD may be a novel hypermethylation agent.

Keywords Myelodysplastic syndrome, Polydatin, Oncogene, Hypermethylation, Hypomethylation

Abbreviations

MDS	Myelodysplastic syndrome
AML	Acute myeloid leukemia
MSCs	Mesenchymal stromal cells
DMSs	Differentially methylated genes
DNMT	DNA methyltransferase
DNMT1	DNA (cytosine-5)-methyltransferase 1
DNMT3a	DNA (cytosine-5)-methyltransferase 3a
DNMT3b	DNA (cytosine-5)-methyltransferase 3b
SAM	S-adenosylmethionine
SALL4	Sal-like protein 4
PIK3CA	Phosphatidylinositol-4,5-bisphosphate 3-kinase catalytic subunit alpha
ITPR3	Inositol 1,4,5-triphosphate receptor 3
SPOPL	Speckle type BTB/POZ protein like

[1]Institute of Geriatric Medicine, Xiyuan Hospital, China Academy of Chinese Medical Sciences, Beijing, China. [2]Institute of Hematology, Xiyuan Hospital, China Academy of Chinese Medical Sciences, Beijing, China. [3]China Academy of Chinese Medical Sciences, Beijing, China. [4]Qingbing Zhou, Yuanbin Liang and Ruofan Chen contributed equally to this work. ✉email: tcmboguanban@126.com; Dr.xufengqin@outlook.com

Myelodysplastic syndrome (MDS) is a category of malignant clonal disorders that stem from hematopoietic stem cells within the bone marrow. These conditions are defined by ineffective blood cell production, persistent cytopenia, and an elevated likelihood of progressing to acute myeloid leukemia (AML)[1]. In the past, MDS was considered to involve hypermethylation[2]. However, emerging studies suggest that aberrant hypomethylation is also a critical factor in MDS pathogenesis. For example, a previous study reported that aberrant hypomethylation of preferentially expressed antigens in the melanoma (*PRAME*) promoter was found in 19.6% of MDS patients, and these patients had a poor prognosis[3]. Moreover, SALL4 is instrumental in the progression of various cancers, functioning as an oncogene[4]. Lin et al. found that 21.7% (18/83) of MDS patients displayed abnormal hypomethylation of the SALL4 gene, which correlated with notably shorter survival rates[5]. In our earlier research, we discovered several hypomethylated genes in a group of five MDS patients in contrast to three healthy donors utilizing the Human Methylation 850 K Bead Chip[6]. However, a larger sample size is required to comprehensively investigate DNA methylation patterns in MDS patients, especially hypomethylated oncogenes.

At present, there is still no cure for MDS except for hemopoietic stem cell transplantation, and most patients eventually die from fatal infection and bleeding caused by cytopenia and acute leukemia[7]. Several studies have emphasized the crucial role of abnormal DNA methylation in the pathologic development of MDS[8]. Over the last two decades, the use of the demethylation agents azacitidine and decitabine, which mainly target abnormal hypermethylation, has greatly progressed the treatment of MDS, especially high-risk MDS[9]. However, a real-world clinical study revealed that the median survival for high-risk MDS patients receiving azacytidine treatment was limited to 18 months[10]. Therefore, these agents fail to fully address the clinical needs of MDS patients, highlighting the urgent need for novel hypomethylation-targeting therapies to achieve improved therapeutic outcomes.

Recently, emerging bioactive compounds derived from traditional Chinese herbal medicine have shown potential as a solution to overcome the limitations of current MDS treatments[6]. Polydatin (PD), a polyphenolic compound extracted from *Polygoni Cuspidati Rhizoma et Radix*, has been reported to inhibit the proliferation of multiple tumor cell types, such as osteosarcoma, colorectal cancer, and hepatocellular carcinoma cells[11–13]. However, no studies have reported how PD affects DNA methylation in MDS cells. Here, we hypothesized that PD targets the aberrant hypomethylation in MDS. To prove this hypothesis, we began this study by utilizing the GEO database to examine DNA methylation patterns in MDS patients, using a sample size larger than that in our previous research. Then, we assessed the genome-wide changes in DNA methylation induced by PD treatment in these cells. Kyoto Encyclopedia of Genes and Genomes (KEGG) was used to analyze those PD-induced hypermethylated genes. Western blotting (WB) was carried out to observe the effects of PD on DNA methyltransferases (DNMTs) in both SKM-1 and MUTZ-1 cells. Furthermore, the key hypermethylated genes induced by PD were identified using Cytoscape 3.10.2, and their protein expression levels were determined via WB. Finally, we performed assays using a Cell Counting Kit-8 (CCK-8) and flow cytometry to evaluate the impact of PD treatment on MDS cells.

Materials and methods
Reagents and cell lines
PD was obtained from the National Institutes for Food and Drug Control. A stock solution was prepared by dissolving PD in DMSO. A Cell Counting Kit-8 (# E1CK000208-10, EnoGene, Nanjing, China) was used to determine cell viability. Detection of cell cycle distribution and apoptosis was performed using a Cell Cycle and Apoptosis Analysis Kit (# C1052) and an Annexin V-FITC Apoptosis Detection Kit (# p0013B) from Beyotime, in Hangzhou, China. The DNA Extraction Kit (# Y5-69,506) was purchased from Qiagen, Germany. EZ DNA methylation kit (# D5005) was from Zymo Research, USA. The protein extraction kit (# GPP1815) was obtained from Gene Pool, China. Specific primary antibodies and secondary antibodies were sourced from Abcam (Cambridge, USA), Proteintech (Rosemont, USA), and Bioss (Beijing, China). The MDS cell line SKM-1 was a gift from Professor Su-ning Chen at Soochow University. The MUTZ-1 cell line was sourced from Jennio Biotech Co., Ltd. (Guangzhou, China).

DNA methylation information acquisition and analysis
The DNA methylation profiles of 17 MDS patients and 14 healthy donors were downloaded from GEO online database (GSE124390, GSE119617; https://www.ncbi.nlm.nih.gov/). The human samples were all mesenchymal stromal cells (MSCs) and were analyzed using the Illumina Infinium Methylation EPIC BeadChip 850 k. The selected data passed the quality control. Gene annotation was performed via the R package Bioconductor.

DNA extraction and methylation detection
The SKM-1 cells were divided into a DMSO control group (MDS cells treated with DMSO) and a 30 μmol/L PD group (MDS cells treated with DMSO and PD at 30 μmol/L). Following 72 h of treatment, cells were collected. Genomic DNA was immediately extracted using a Qiagen DNeasy Blood & Tissue Kit in accordance with the product's guidelines. The Illumina Infinium Methylation EPIC BeadChip 850 k was subsequently used to detect the methylation status of the DNA samples. Briefly, the bisulfite DNA was conversed with an EZ DNA methylation kit according to the product's instruction manual. Following amplification, fracture, precipitation and resuspension, the DNA was hybridized and washed. An SQ fluorescence scanner was used to scan the DNA. The degree of DNA methylation was then calculated from the raw signal values to obtain the original beta value matrix. The beta value is a commonly used index to measure a DNA methylation site ranging from 0–1. As the beta value approaches 1, DNA methylation increases; as it nears 0, methylation decreases. The β value was calculated using the following formula:

$$beta_i = \frac{\max\left(y_{(i,methy)},0\right)}{\max\left(y_{(i,methy)},0\right) + \max\left(y_{(i,unmethy)},0\right) + 100}$$

Bioinformatics analyses

The hypomethylated genes of MDS patients vs. healthy donors and hypermethylated genes induced by PD were analyzed via KEGG pathway enrichment using the DAVID platform for bioinformatics. The criterion was set as P<0.05, and the top 30 pathways and functions are listed. Protein-protein interaction (PPI) network construction was carried out by STRING (https://string-db.org/), and then the key genes were obtained and visualized utilizing Cytoscape 3.10.2 (https://cytoscape.org/).

Western blotting

The two cell lines were divided into three groups: DMSO control group (MDS cells treated with DMSO), 10 µmol/L group (DMSO and PD at 10 µmol/L), and 30 µmol/L group (DMSO and PD and 30 µmol/L). Proteins extraction was conducted by a protein extraction kit following the product's instructions. After performing SDS-PAGE, proteins were transferred to a PVDF membrane and incubated with the primary antibodies: anti-Dnmt3b (Abcam/ab79822, 1:500), anti-Dnmt3a (Abcam/ab188470, 1:500), anti-Dnmt1 (Abcam/ab188453, 1:500), anti-PIK3CA (Bioss/bs2067R, 1:500), anti-ITPR3 (Proteintech/20,729–1-Ig, 1:500), anti-SPOPL (Proteintech/17,740–1-Ig, 1:500), and anti-Actin (Abcam/ab8226, 1:3000) /anti-GAPDH (Abcam/ab181602, 1:3000). Afterward, the membranes were incubated with goat anti-rabbit IgG HRP (Abcam/ab6721, 1:5000). The antigen-antibody complexes were detected using enhanced chemiluminescence (ECL) reagents (Thermo Fisher, USA) in a dark room. The total grayscale value of each protein band was quantified via Quantity One v.4.6.2.

CCK-8 cell viability assay

SKM-1 and MUTZ-1 cells were grown and maintained in RPMI-1640 medium containing 10% fetal bovine serum (Gibco, California, USA) under standard culture conditions. Then the cells were seeded at a density of 2×10^5 cells per well in 96-well plates. PD was added at final concentrations of 0, 25, 50, 100, and 200 µmol/L. Following 72 h of incubation, CCK-8 reagent (10µL) was added, followed by incubation for 1 h. The absorbance at 460 nm was assessed utilizing a microplate reader (Biotek, Shanghai, China). The experiment was repeated three times, with five replicates each time, and the cell viability of each group was calculated.

Cell cycle distribution and apoptosis assays

The exponentially growing phase cells were adjusted to a density of 2×10^5 cells/mL. There were three groups of cells: a blank group (MDS cells only), a DMSO control group (MDS cells treated with DMSO), a 10 µmol/L group (MDS cells treated with DMSO and PD at 10 µmol/L), and a 30 µmol/L group (MDS cells treated with DMSO and PD at 30 µmol/L). Following 72 h of incubation, the cells were harvested for cell cycle and apoptosis assays. The cells were fixed with 75% cold ethanol at 4 °C overnight for cell cycle distribution detection, after which the ethanol was removed, and the mixture was stained with a mixture of propidium iodide (PI) staining solution for 30 min in the dark. For cell apoptosis detection, Annexin V-FITC binding solution, PI, and Annexin V-FITC were added to the tubes in sequence and incubated with the cells for 10 min in the dark. Apoptosis and the cell cycle were analyzed by a flow cytometer (Beckman Coulter, USA). Replicate experiments were conducted to confirm the findings. Wright staining was performed to observe SKM-1 cell morphology.

Statistical analysis

T-test and one-way ANOVA with the Bonferroni post-hoc test were performed to compare cell cycle distribution, apoptosis distribution and protein expression among different groups, considering $p < 0.05$ as statistically significant. For the methylation data, Bayesian and linear regression approaches were applied, differences in DNA methylation among different groups for SKM-1 cells were evaluated using a threshold of ± 0.06, and a p value <0.01 was set as the significance criterion. Statistical analyses were performed on data from at least three independent experiments.

Results

Abnormal gene hypomethylation is common in MDS patients

To observe the methylation characteristics of MDS patients, we compared MSCs derived from seventeen MDS patients and fourteen healthy donors utilizing human methylation chip data from the GEO database. Numerous differentially methylated sites (DMSs) were identified in MDS patients, and the top 1000 DMSs are shown in a heatmap (Fig. 1a). We identified 5491 aberrantly hypomethylated sites and 14,759 aberrantly hypermethylated sites (Fig. 1b). KEGG pathway analysis revealed that several pathways related to cancer, such as PI3K-AKT signaling pathway and MAPK signaling pathway (Fig. 1c). Furthermore, PPI analysis revealed that the key hypomethylated genes in MDS included PIK3CA, RAP1, and PKT (Fig. 1d).

PD induces hypermethylation in SKM-1 cells on a genome-wide scale

We utilized the Infinium Human Methylation 850 K BeadChip to assess whole-genome methylation changes in SKM-1 cells following treatment with PD. The heatmap indicated a significantly higher genome-wide methylation level in the PD-treated group compared to the DMSO control group (Fig. 2a). The volcano plot shows the DMSs between the two groups (Fig. 2b). We found that the methylation of 623 genes was notably altered by PD treatment (Tables S1 and S2), among which 448 genes (71.91%) were hypermethylated. Several pathways related to cancer, such as PI3K-AKT signaling pathway, mTOR signaling pathway, and the cGMP-PKG signaling pathway, were enriched in these hypermethylation genes (Fig. 2c).
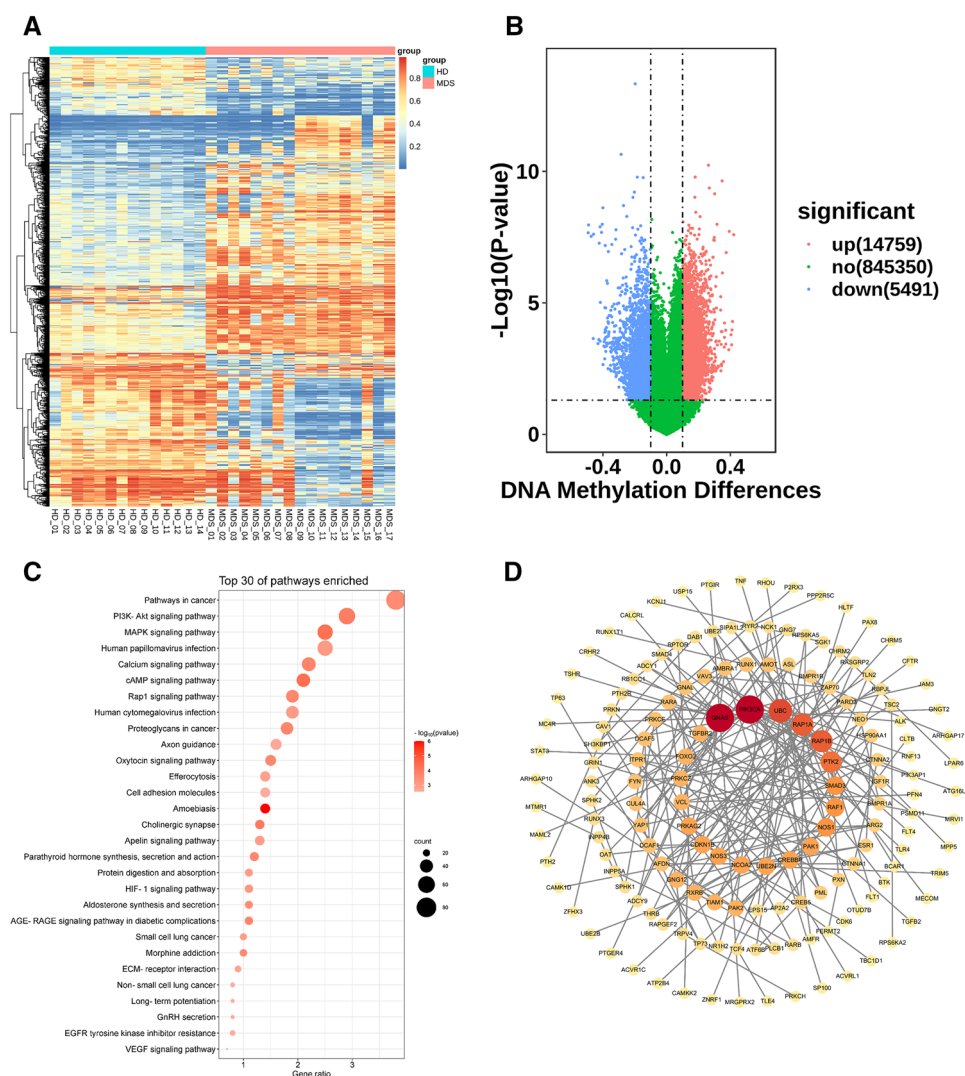
Fig. 1. The 850 K BeadChip DNA methylation data revealed an aberrant methylation pattern in 17 MDS patients compared with 14 healthy donors. (**A**) Heatmap of the top 1000 DMSs ranked by differential values, comparing MDS patients to healthy donors. (**B**) Volcano plot of the DMSs between MDS patients and healthy donors. Red (up) represents the hypermethylated sites, and blue (down) represents the hypomethylated genes. (**C**) KEGG pathway enrichment analysis of differentially hypomethylated genes in MDS patients compared with healthy donors. (**D**) PPI network analysis of differentially hypomethylated genes in MDS patients; the size and intensity of the nodes correspond to the degree of interaction, with larger and darker nodes indicating higher degree values.

PD increases the protein expression of DNMTs in SKM-1 and MUTZ-1 cells

Following PD treatment, the protein expression levels were examined in MDS cells, including DNMT1, DNMT3a, and DNMT3b (Fig. 3a). For SKM-1 cells, PD treatment at 30 µmol/L significantly increased the expressions of DNMT1, DNMT3a, and DNMT3b ($p < 0.05$), whereas the expressions of DNMTs did not change after PD treatment at 10 µmol/L when comparing with those in DMSO control group respectively ($p > 0.05$). (Fig. 3b). In MUTZ-1 cells (Fig. 3c), PD treatment at 30 µmol/L significantly increased the expression of DNMT1 and DNMT3b ($p < 0.05$), whereas no change existed of the expression of DNMT3a in both PD treatment groups versus DMSO control group ($p > 0.05$).

PD inhibits the protein expression of PIK3CA, ITPR3 and SPOPL in SKM-1 cells

Among the 448 hypermethylated genes induced by PD, hub hypermethylated genes including *PIK3CA, SPOPL* and *ITPR3*, were identified and marked in red using Cytoscape 3.10.2 (Fig. 4a).

DNA methylation is known to inhibit gene transcription. In this study, the expression levels of the oncogenes PIK3CA, ITPR3, and SPOPL were examined in SKM-1 cells following PD treatment (Fig. 4b). PD treatment at 10 and 30 µmol/L significantly decreased the expression of PIK3CA ($p < 0.01$) and ITPR3 ($p < 0.05$; Fig. 4c & d). The expression of SPOPL remained unchanged after PD treatment at 10 µmol/L, whereas treatment at 30 µmol/L significantly inhibited SPOPL expression compared with that in the DMSO control group ($p < 0.05$) (Fig. 4e).
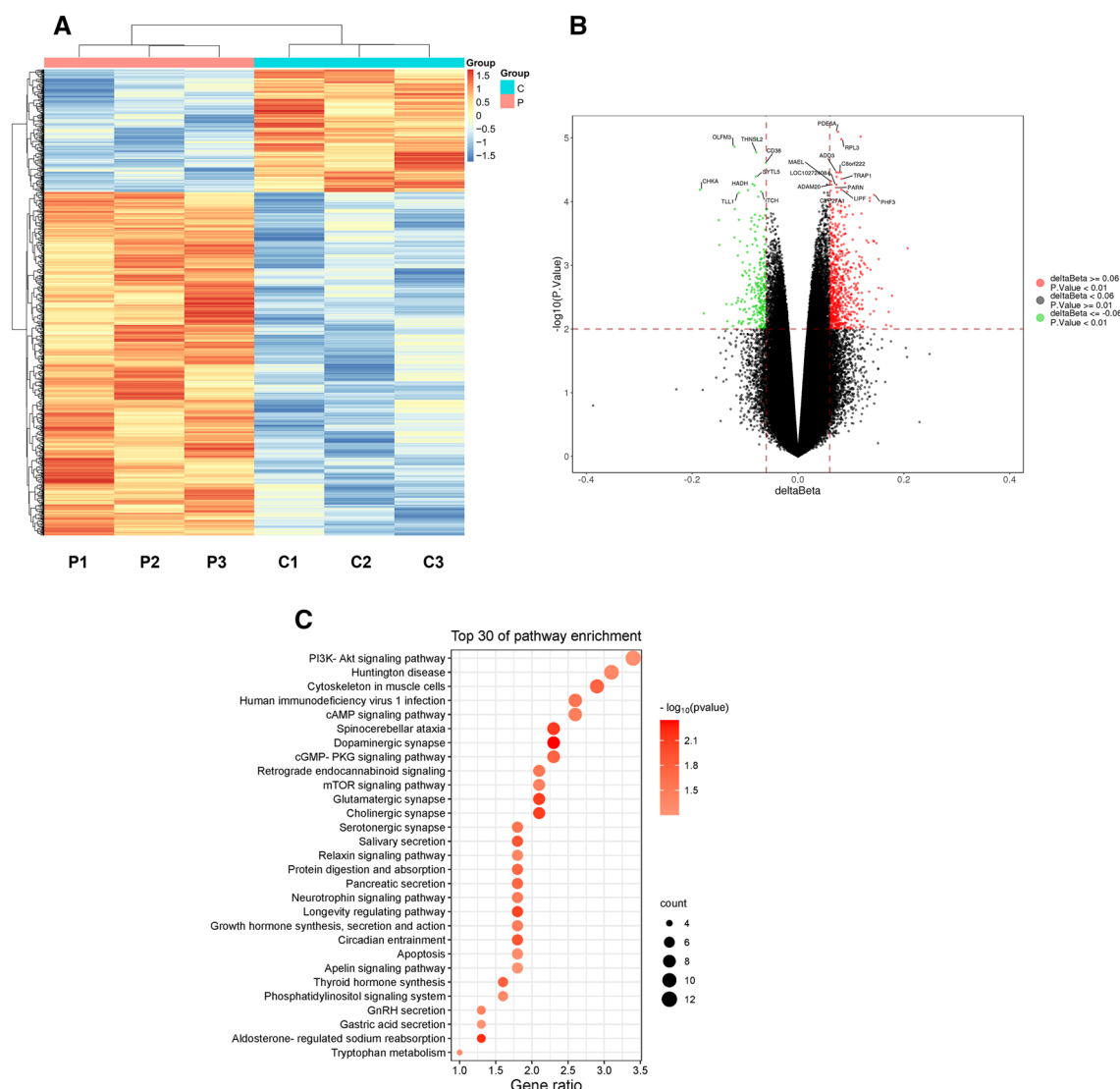
Fig. 2. The 850 K BeadChip DNA methylation data revealed the effects of PD on gene methylation in SKM-1 cells. (**A**) Heatmap depicting the median methylation level at CpG sites between the DMSO control group and the PD-treated group, with red representing the PD treatment group (P1–P3) and blue representing the DMSO control group (C1–C3). (**B**) Volcano plot illustrating CpG methylation in genes of the PD group compared with those of the DMSO control group. The red vertical dotted line delineates ± 0.06 in the Beta value between the two groups, and the horizontal dotted line represents a *p* value threshold of 0.01. Hypermethylated genes (448) are shown in red, and hypomethylated genes (175) are shown in green. (**C**) The top 30 enriched pathways of the hypermethylated genes induced by PD treatment.

PD inhibits the proliferation of SKM-1 and MUTZ-1 cells

Figure 5a illustrates the chemical structure of PD, which was provided by the National Institutes for Food and Drug Control. SKM-1 and MUTZ-1 cells were incubated with PD at 0 to 200 μM for 72 h. Figure 5b shows the dose-dependent inhibitory effect of PD on the viability of the two cell lines.

PD induces S-phase cell cycle arrest in SKM-1 and MUTZ-1 cells

Cell cycle analysis demonstrated that PD treatment altered the cell cycle distribution of SKM-1 and MUTZ-1 cells (Fig. 6a, b). The cell cycle distribution of the two cell lines in DMSO control group was similar to that in the blank group ($p > 0.05$). When PD was added at different concentrations, the proportion of cells in the S phase significantly changed in MUTZ-1 cells (control: $33.70 \pm 2.07\%$; 10 μmol/L: $47.93 \pm 3.02\%$; 30 μmol/L: $61.57 \pm 2.20\%$) and cells in the G0/G1 phase significantly decreased (control: $57.27 \pm 2.75\%$; 10 μmol/L: $39.77 \pm 1.62\%$; 30 μmol/L: $25.43 \pm 0.39\%$) ($p < 0.0001$; Fig. 6c). In SKM-1 cells, treatment with two concentrations of PD resulted in a more pronounced effect on the cell arrest in the S phase ($p < 0.0001$; Fig. 6d). These results indicate that PD induces S-phase arrest, partially blocking DNA replication and cell cycle progression.
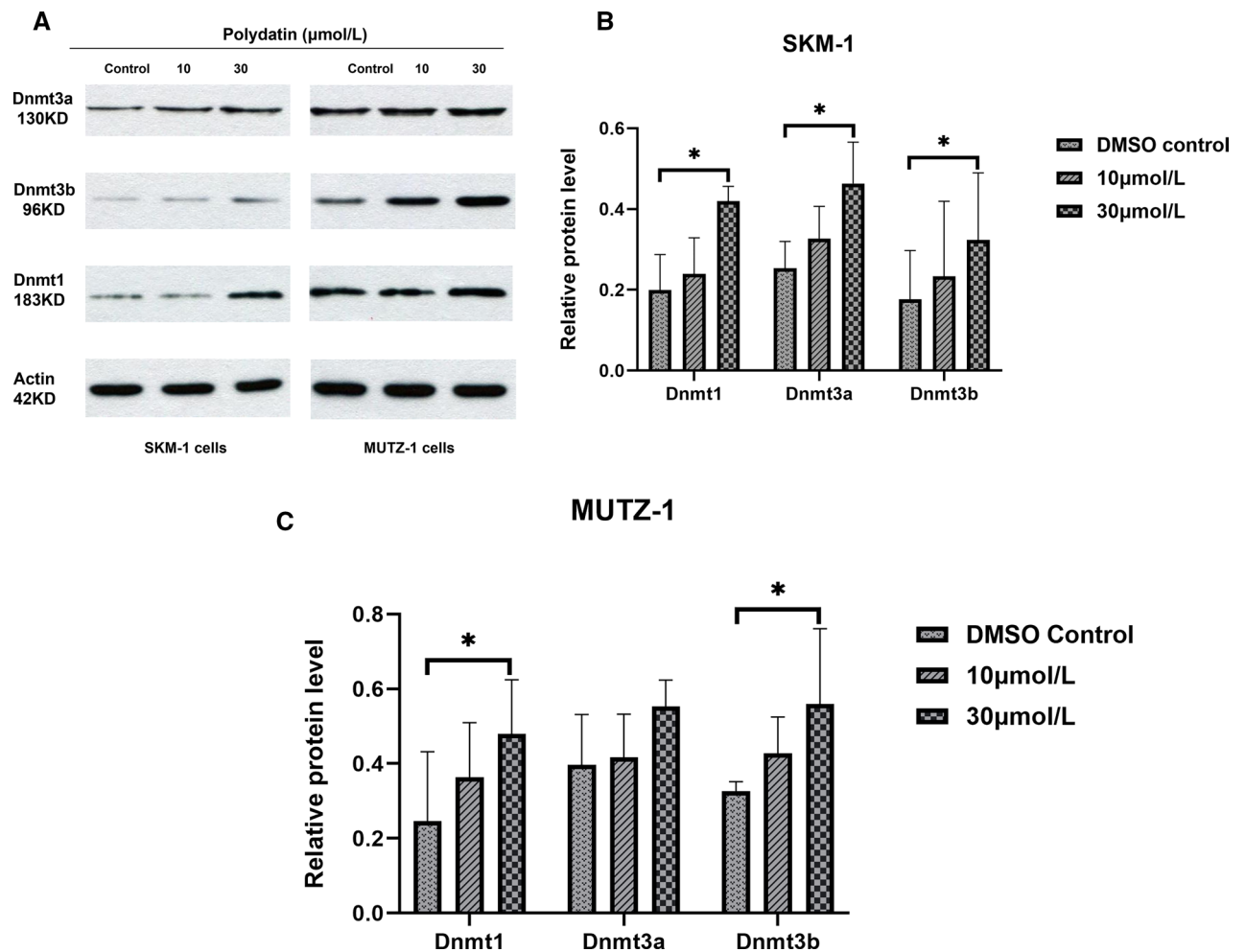
Fig. 3. PD increased the protein expression of DNA methyltransferases (DNMTs), including DNMT1, DNMT3a and DNMT3b, in SKM-1 and MUTZ-1 cells. (**A**) The expression levels of DNMT1, DNMT3a and DNMT3b following PD treatment for 48 h. (**B**) and (**C**) Grayscale values of DNMT1, DNMT3a and DNMT3b in SKM-1 and MUTZ-1 cells. $*p < 0.05$, n = 3.

PD induces apoptosis in SKM-1 and MUTZ-1 cells

PD treatment notably increased the proportion of apoptotic cells (Fig. 7a). For example, the percentage of viable apoptotic SKM-1 cells increased from $0.26 \pm 0.03\%$ (DMSO control) to $3.83 \pm 0.03\%$ (PD at 30 μmol/L) ($p < 0.0001$), and change of nonviable apoptotic cells was similar (Fig. 7b). In MUTZ-1 cells, nonviable apoptosis increased significantly from $2.7 \pm 1.11\%$ (DMSO control) to $6.07 \pm 0.65\%$ with 10 μmol/L PD treatment ($p < 0.05$) and further increased to $9.80 \pm 1.16\%$ with 30 μmol/L PD ($p < 0.0001$; Fig. 7c). The pathological morphologies of SKM-1 cells in each group were shown in Fig. 7d. In both the 10 μmol/L group and 30 μmol/L group, apoptotic SKM-1 cells were identified. Wright staining revealed that the apoptotic cell had a reduced size, pyknotic nuclei, and was accompanied by apoptotic bodies.

Discussion

In this study, genome-wide DMGs were identified in 17 MDS patients compared with 14 healthy donors utilizing data from the GEO online database and revealed several aberrantly hypomethylated genes. Bioinformatic analysis revealed that various cancer related pathways such as the PI3K-AKT signaling pathway and the MAPK signaling pathway were significantly enriched in these hypomethylated genes. The PPI network revealed hub hypomethylated genes including *GNAS*, *PIK3CA*, and *RAP1*. These pathways and hub genes play critical roles in MDS. For example, activation of the PI3K-AKT signaling pathway has been shown in CD34 + cells from MDS patients[14]. Taken together, the data from the GEO database strongly indicate that drugs targeting aberrant hypomethylation, distinct from present hypomethylating agents, may be essential for future MDS treatment, particularly in patients unresponsive to currently employed hypomethylating therapies.

Targeting aberrant hypermethylation with DNA hypomethylating agents (HMAs) has been a significant advancement in the treatment of MDS. However, the failure of HMAs remains common, and there are no curative therapies outside of allogeneic hematopoietic stem cell transplantation[15,16]. Considering the key role of abnormal hypomethylation in MDS, novel drugs for DNA hypomethylation-targeted therapy may be needed to improve
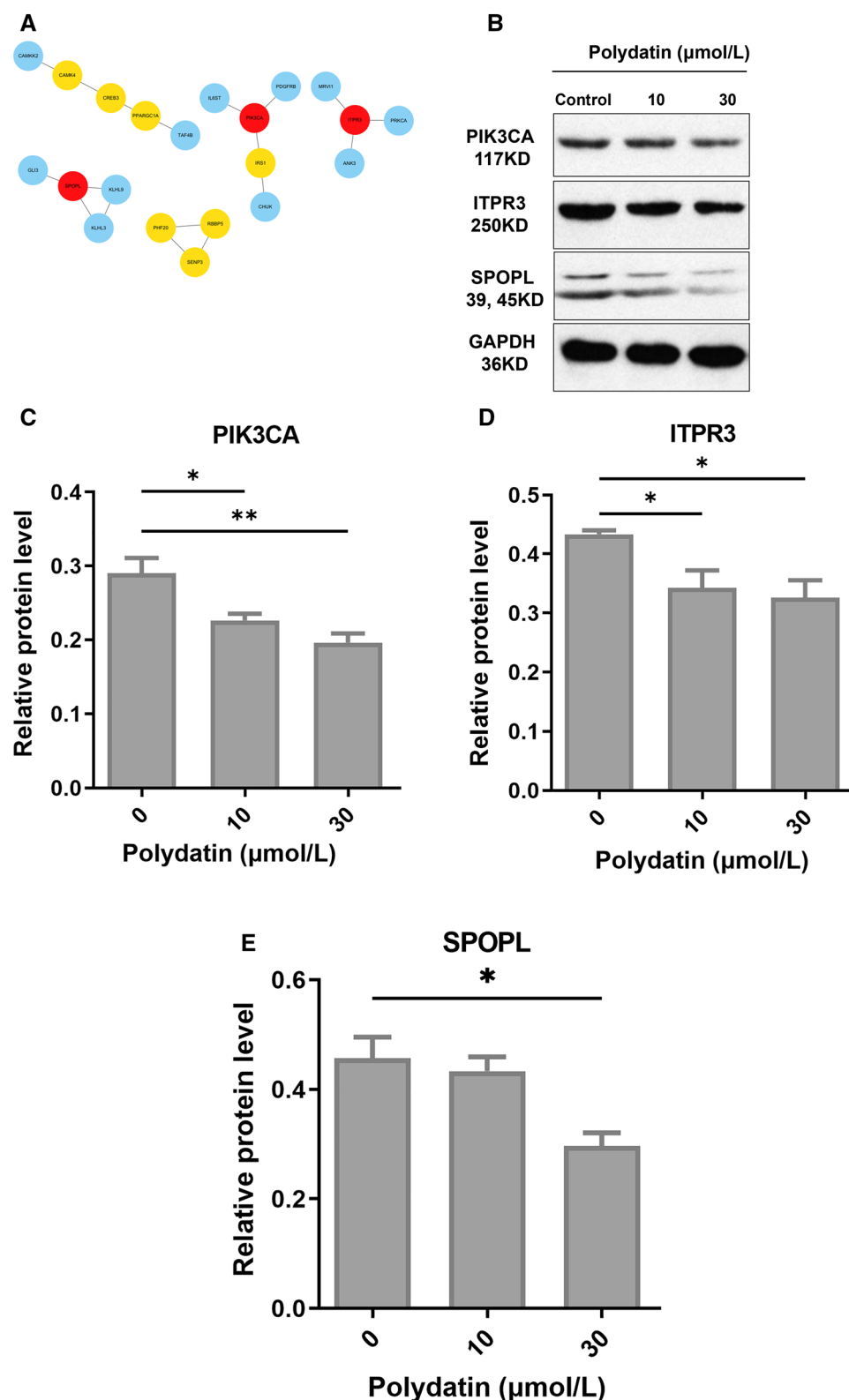
Fig. 4. PD inhibited the protein expression of PIK3CA, ITPR3 and SPOPL in SKM-1 cells. (**A**) A PPI network constructed via the STRING database and visualized by Cytoscape. PIK3CA, ITPR3 and SPOPL were identified as the hub genes in red. (**B**) Protein expression bands of PIK3CA, ITPR3 and SPOPL following PD treatment for 48 h. Grayscale values of PIK3CA (**C**), ITPR3 (**D**) and SPOPL (**E**). *$p < 0.05$, **$p < 0.01$.
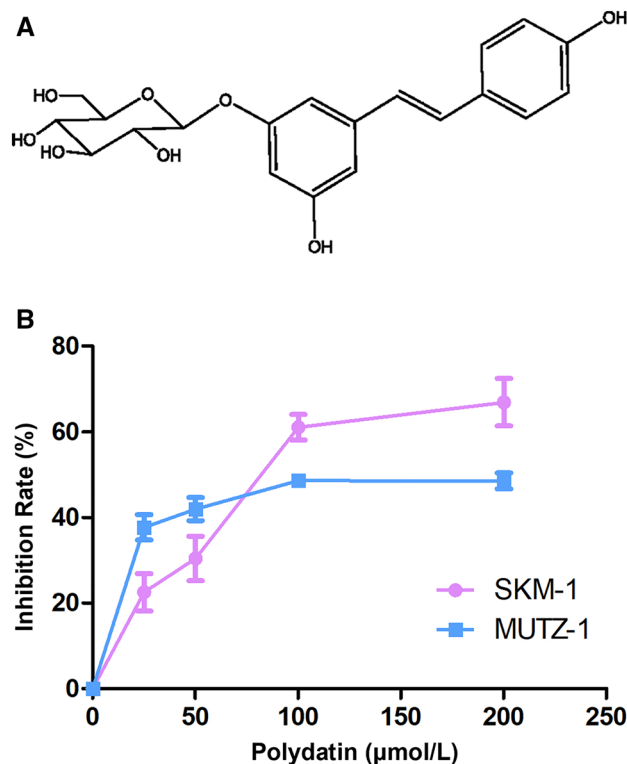
Fig. 5. PD reduces the viability of SKM-1 and MUTZ-1 cells. (A) Chemical structure of PD. (B) Dose–response curves for the proliferation of SKM-1 and MUTZ-1 cells after treatment with PD for 48 h. The error bars represent the means ± SEMs, n = 3.

the clinical efficacy of MDS treatment. Interestingly, the present study indicated that PD acts as a methylation-promoting agent. Human methylation chip analyses identified 623 DMGs following PD treatment, of which 448 genes (71.91%) were hypermethylated. These hypermethylated genes were associated primarily with pathways such as the PI3K-AKT signaling pathway, cGMP-PKG signaling pathway, and glutamatergic pathway. DNA methylation involves the covalent addition of a methyl group from S-adenosylmethionine (SAM) to cytosine, which is mainly mediated by DNMTs[17]. To further investigate the mechanism of PD hypermethylation, WB was performed to assess the effect of PD on three DNMTs protein expression in two MDS cell lines. In SKM-1 cells, compared with DMSO treatment, PD treatment effectively increased the expression of DNMT1, DNMT3a and DNMT3b. In MUTZ-1 cells, PD treatment significantly elevated DNMT1 and DNMT3b protein levels. These findings suggest that PD promotes genome-wide DNA methylation by increasing DNMTs expression, highlighting its potential as an innovative hypermethylation agent.

Hypermethylation in promoter regions suppresses gene expression, whereas hypomethylation can lead to gene overexpression. In this study, we applied Cytoscape analysis to determine the core hypermethylated genes induced by PD. The results revealed that *PIK3CA*, *ITPR3* and *SPOPL* were key genes in the network, all of which are classified as oncogenes. *PIK3CA* is a key molecule in the PI3K-AKT signaling pathway and plays a pivotal role in tumor cell proliferation, apoptosis, migration and blood vessel generation. *PIK3CA* is well known as an oncogene and recognized as a potential therapeutic target in multiple cancers[18–20]. Similarly, *ITPR3* is also a driver oncogene, frequently overexpressed in cancers like glioblastoma, squamous cell carcinoma, colorectal cancer and cholangiocarcinoma. High expression of *ITPR3* is associated with adverse clinical outcomes, making it an attractive therapeutic target in cancer treatment[21–24]. Notably, WB analysis revealed that PD treatment inhibited the protein expression level of these three oncogenes in SKM-1 cells. These findings suggest that PD promotes the DNA methylation of oncogenes, subsequently downregulating their expression, which may represent the primary mechanism underlying its therapeutic effects.

In malignant diseases, tumor cells are abnormally active, apoptosis is inhibited, and the overexpression of oncogenes can promote proliferation and inhibit apoptosis. For example, PIK3CA can regulate cell survival and proliferation by influencing cell apoptosis[25]. Mutations in *PIK3CA* often lead to aberrant activation of the PI3K/AKT signaling pathway, which contributes to cancer progression by suppressing apoptosis and promoting cell survival[26]. *ITPR3* interacts with proteins such as PTEN and STAT3 to regulate endoplasmic reticulum–mitochondria Ca²⁺ flux, preventing excessive calcium transfer, which can induce apoptosis[27]. *SPOPL* overexpression in glioma stem cells promotes tumorigenicity and stemness by activating the Notch signaling pathway[28]. Our CCK-8 assay results demonstrated PD could notably inhibit the proliferation of MDS cell lines in a dose-dependent manner. Moreover, PD treatment significantly decreased the G0/G1 phase cell proportion while increasing that in the S phase. Additionally, apoptosis detection revealed that PD treatment markedly
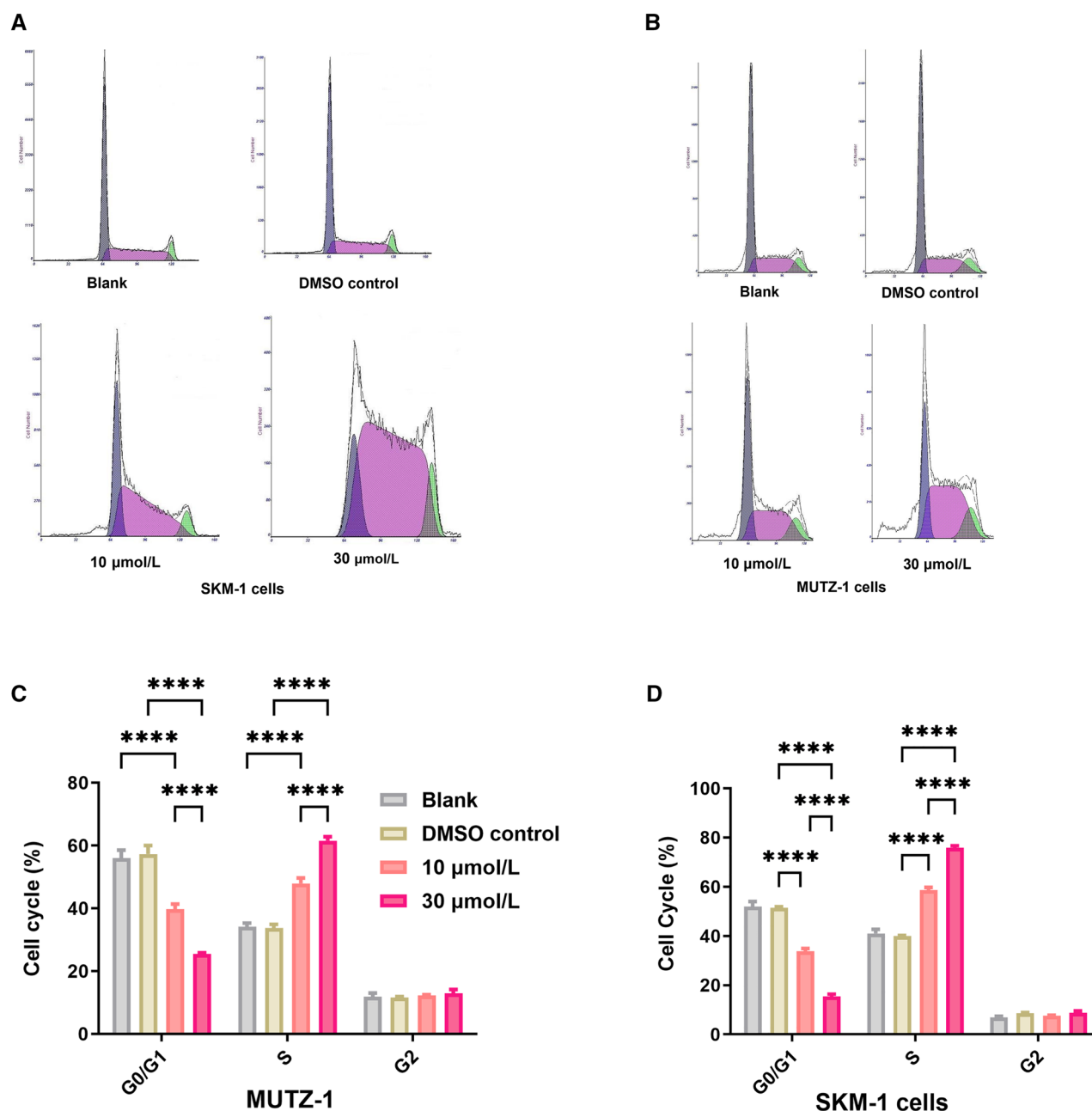
Fig. 6. PD induces S-phase arrest in SKM-1 and MUTZ-1 cells (n = 3). (**A**) and (**B**)Representative flow cytometry images. (**C**) and (**D**) Percentages of SKM-1 and MUTZ-1 cells in each phase of the cell cycle, respectively, after treatment with PD (0, 10, or 30 μmol) for 48 h. The values are expressed as the means ± SEMs. $*p < 0.05$, $****p < 0.0001$.

increased the proportion of apoptotic SKM-1 and MUTZ-1 cells. These findings suggest that PD may have therapeutic effects by downregulating the expression of PIK3CA, ITPR3 and SPOPL.

In summary, our findings demonstrated that hypomethylated genes play a significant role in pathological progression in MDS patients. PD induced the methylation of *PIK3CA*, *ITPR3* and *SPOPL*, decreased the protein expression of these oncogenes, and induced apoptosis in MDS cells. Furthermore, increased protein expression of DNMTs was observed in SKM-1 and MUTZ-1 cells, indicating that PD may be a novel hypermethylation agent. In the future, clinical trials are needed to confirm the improved survival rates and therapeutic efficacy of PD in MDS patients.
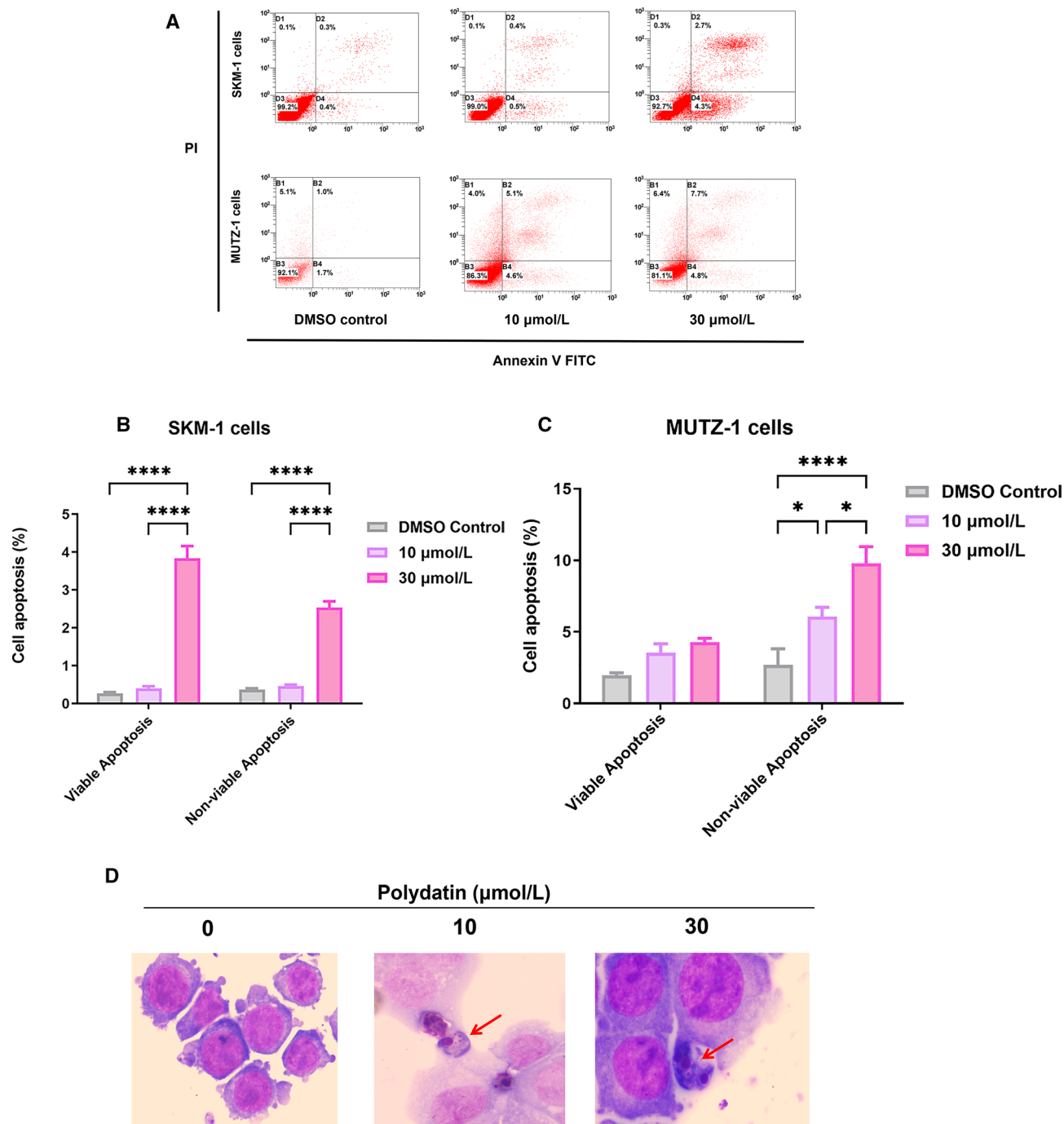
Fig. 7. PD increases the proportions of apoptotitic SKM-1 and MUTZ-1 cells (n = 3). (**A**) Representative flow cytometry images. Apoptotic cell proportions in SKM-1 (**B**) and MUTZ-1 cells (**C**) following treatment with PD (0, 10, and 30 µmol/L) for 48 h. The values are expressed as the means ± SEMs. *$p < 0.05$, ****$p < 0.0001$. PI, propidium iodide. (**D**) Wright-stained images highlighting apoptotic cells (indicated by "↓") observed at 10×100 magnification.

Data availability

The datasets used and/or analysed during the current study are available from the corresponding author on reasonable request.

References

1. Cazzola, M. Myelodysplastic syndromes. *N. Engl. J. Med.* **383**, 1358–1374 (2020).
2. Figueroa, M. E. et al. MDS and secondary AML display unique patterns and abundance of aberrant DNA methylation. *Blood* **114**, 3448–3458 (2009).
3. Qian, J. et al. Hypomethylation of *PRAME* promoter is associated with poor prognosis in myelodysplastic syndrome. *Br. J. Haematol.* **154**, 153–155 (2011).
4. Sun, B., Xu, L., Bi, W. & Ou, W. B. SALL4 oncogenic function in cancers: Mechanisms and therapeutic relevance. *IJMS* **23**, 2053 (2022).
5. Lin, J. et al. Aberrant hypomethylation of SALL4 gene in patients with myelodysplastic syndrome. *Leuk. Res.* **37**, 71–75 (2013).
6. Zhou, Q. et al. Traditional Chinese medicine containing arsenic treated MDS patients effectively through regulating aberrant hypomethylation. *Evidence-Based Complementary Alternative Med.* **2020**, 7469809 (2020).
7. Nachtkamp, K., Kobbe, G., Gattermann, N. & Germing, U. Myelodysplastic syndromes: New methods of diagnosis, prognostication, and treatment. *Dtsch Arztebl Int.* **120**, 203–210 (2023).
8. Feng, Y. et al. Analysis of core mutation and TET2/ASXL1 mutations DNA methylation profile in myelodysplastic syndrome. *Hematology* **28**, 2220222 (2023).
9. Gerke, M. B., Christodoulou, I. & Karantanos, T. Definitions, biology, and current therapeutic landscape of myelodysplastic/myeloproliferative neoplasms. *Cancers* **15**, 3815 (2023).
10. Mozessohn, L. et al. Azacitidine in the 'real-world': An evaluation of 1101 higher-risk myelodysplastic syndrome/low blast count acute myeloid leukaemia patients in ontario, canada. *Br. J. Haematol.* **181**, 803–815 (2018).
11. Chen, Q. et al. Polydatin increases radiosensitivity by inducing apoptosis of stem cells in colorectal cancer. *Int. J. Biol. Sci.* **15**, 430–440 (2019).
12. Jiang, J. et al. Erratum: Polydatin inhibits hepatocellular carcinoma via the AKT/STAT3-FOXO1 signaling pathway. *Oncol. Lett.* **18**, 5654 (2019).
13. Jiang, C. et al. Polydatin induces apoptosis and autophagy via STAT3 signaling in human osteosarcoma MG-63 cells. *J. Nat. Med.* **74**, 533–544 (2020).
14. Rezende, D. C. et al. PI3K/AKT pathway as a potential therapeutic target in myelodysplastic syndrome. *Blood* **116**, 1871–1871 (2010).
15. Alain, M. et al. Advancing drug development in myelodysplastic syndromes. *Blood Adv.* **9**, 1095–1104 (2025).
16. Farzad Teymouri, Constantin A. Teymouri, F. & Dasanu, C. A. Selecting optimal therapy for higher-risk myelodysplastic syndromes: Present and future projections. *Expert Opin Pharmacother.* **26**, 345–347 (2025).
17. Portela, A. & Esteller, M. Epigenetic modifications and human disease. *Nat. Biotechnol.* **28**, 1057–1068 (2010).
18. Li, X., Zhang, R., Liu, Z., Li, S. & Xu, H. The genetic variants in the PTEN/PI3K/AKT pathway predict susceptibility and CE(A)F chemotherapy response to breast cancer and clinical outcomes. *Oncotarget* **8**, 20252–20265 (2017).
19. Wang, Q. et al. PIK3CA mutations confer resistance to first-line chemotherapy in colorectal cancer. *Cell Death Dis.* **9**, 739 (2018).
20. Marquard, F. E. & Jücker, M. PI3K/AKT/mTOR signaling as a molecular target in head and neck cancer. *Biochem. Pharmacol.* **172**, 113729 (2020).
21. Kang, S. S. et al. Caffeine-mediated inhibition of calcium release channel inositol 1,4,5-trisphosphate receptor subtype 3 blocks glioblastoma invasion and extends survival. *Can. Res.* **70**, 1173–1183 (2010).
22. Shibao, K. et al. The type III inositol 1,4,5-trisphosphate receptor is associated with aggressiveness of colorectal carcinoma. *Cell Calcium* **48**, 315–323 (2010).
23. Yang, Y. C. et al. *ITPR3* gene haplotype is associated with cervical squamous cell carcinoma risk in taiwanese women. *Oncotarget* **8**, 10085–10090 (2017).
24. Ueasilamongkol, P. et al. Type 3 inositol 1,4,5-trisphosphate receptor is increased and enhances malignant properties in cholangiocarcinoma. *Hepatology* **71**, 583–599 (2020).
25. Janku, F., Yap, T. A. & Meric-Bernstam, F. Targeting the PI3K pathway in cancer: Are we making headway?. *Nat. Rev. Clin. Oncol.* **15**, 273–291 (2018).
26. Dumbrava, E. E. et al. PIK3CA mutations in plasma circulating tumor DNA predict survival and treatment outcomes in patients with advanced cancers. *ESMO Open* **6**, 100230 (2021).
27. Avalle, L. et al. STAT3 localizes to the ER, acting as a gatekeeper for ER-mitochondrion Ca2+ fluxes and apoptotic responses. *Cell Death Differ.* **26**, 932–942 (2019).
28. Hu, T., Xuan, R., Han, E., Cai, L. & Xia, Z. SPOPL induces tumorigenicity and stemness in glioma stem cells by activating notch signaling. *J. Neurooncol.* **164**, 157–170 (2023).

Acknowledgements

Author contributions

Qingbing Zhou: Methodology, writing original draft. Yuanbin Liang: Data analysis, manuscript writing. Ruofan Chen: Writing original draft. Hongzhi Wang: Morphology. Qiuyue Guo and Liu Li: Validation. Xiaobo Zhu and Fengqin Xu: Supervision, methodology. All authors reviewed the manuscript.

Funding

Declarations

Competing interests

The authors declare no competing interests.

Additional information

Supplementary Information The online version contains supplementary material available at https://doi.org/10.1038/s41598-025-01867-6.

Correspondence and requests for materials should be addressed to X.Z. or F.X.

Reprints and permissions information is available at www.nature.com/reprints.

Publisher's note Springer Nature remains neutral with regard to jurisdictional claims in published maps and institutional affiliations.